



## **Biophysical Methods for the Elucidation of the S-Layer Proteins/Metal Interaction**

**Pablo Mobili<sup>1</sup>, Maria de los Angeles Serradell<sup>2</sup>, Claudine Mayer<sup>3,4,5</sup>,  
Véronique Arluison<sup>6,7,8</sup> and Andrea Gomez-Zavaglia<sup>1\*</sup>**

<sup>1</sup>*Centro de Investigación y Desarrollo en Criotecología de Alimentos (Conicet La Plata, UNLP), 1900 La Plata, Argentina.*

<sup>2</sup>*Laboratorio de Microbiología, Departamento de Ciencias Biológicas, Facultad de Ciencias Exactas, Universidad Nacional de La Plata, 47 y 115, 1900 La Plata, Argentina.*

<sup>3</sup>*Département de Biologie Structurale et Chimie, Institut Pasteur, 75015 Paris, France.*

<sup>4</sup>*UMR 3528, CNRS, 75015 Paris, France.*

<sup>5</sup>*Université Paris Diderot, Sorbonne Paris Cité, Cellule Pasteur, 75015 Paris, France.*

<sup>6</sup>*Université Paris Diderot, PRES Sorbonne-Paris Cité, 75205 Paris Cedex 13, France.*

<sup>7</sup>*Laboratoire Jean Perrin FRE 3231 CNRS/Paris 6.*

<sup>8</sup>*Laboratoire Léon Brillouin, UMR12 CEA/CNRS, Commissariat à l'Energie Atomique, 91191 Gif sur Yvette, France.*

### **Authors' contributions**

*This work was carried out in collaboration between all authors. Authors PM, MDLAS, CM, VA and AGZ wrote the manuscript and managed the literature searches. All authors read and approved the final manuscript.*

**Research Article**

**Received 30<sup>th</sup> October 2012**  
**Accepted 10<sup>th</sup> January 2013**  
**Published 19<sup>th</sup> February 2013**

### **ABSTRACT**

Surface-layers (S-layers) are macromolecular paracrystalline arrays of proteins or glycoproteins that can self-assemble into 2-dimensional semi-permeable meshworks to overlay the cell surface of many bacteria and archaea. They usually assemble into lattices with oblique, square or hexagonal symmetry and serve as an interface between the bacterial cell and the environment. Isolated S-layers can recrystallize into two-dimensional regular arrays in suspension or on various surfaces, thus being an appropriate material for several bionanotechnological purposes. Promising applications of S-layers include their use as biotemplates for the capture of metal ions or the synthesis of metal nanoclusters.

\*Corresponding author: Email: [angoza@qui.uc.pt](mailto:angoza@qui.uc.pt);

Considering the use of S-layers as biotemplates for the organization of metal ions or metallic nanoclusters, research on potential of surface layer proteins (SLP) and metals can be understood as an interdisciplinary field, in which different biophysical techniques supply complementary information. In this review, we discuss the SLP as native or engineered “bottom-up” building blocks for metal immobilization structures. We also describe the biophysical techniques used to analyze metal binding properties as well as the information obtained from the investigation of these structures.

**Keywords:** Protein self-assembly; metal ions biosorption; biomineralization; nanobiotechnology.

## ABBREVIATIONS

*S-layers:* Surface-layers; *SLP(s):* Surface layer protein(s); *AFM:* Atomic Force Microscopy; *(cryo-) TEM:* (Cryo-) transmission electron microscopy; *FTIR:* Fourier transform infrared spectroscopy; *NR:* Neutron reflectometry; *QCM:* Quartz crystal microbalance; *SAXS:* Small Angle X-ray scattering; *SPR:* Surface Plasmon Resonance; *TRLFS:* Time resolved induced laser fluorescence spectroscopy; *XAS:* X-ray absorption spectroscopy.

## 1. INTRODUCTION

Surface Layers (S-layers) form the outermost cell envelope of most archaea and many bacteria. S-layers are usually composed of multiple copies of a single protein subunit self-assembled to form a continuous paracrystalline lattice with oblique, tetragonal or hexagonal architectures (Fig. 1), but in some bacteria such as in *Clostridium difficile* the lattice can comprise different subunits [1]. Self-assembly consists of a spontaneous entropy-driven process [2] and the size of each unit cell ranges from 2.5 to 35 nm, whereas the thickness of the layer varies between 5 to 70 nm [3]. S-layer proteins (SLP) represent up to 15 % of the total protein content of the cell and exhibit a high content of hydrophobic amino acids (~50 %), glutamic and aspartic acids (~15 %) and lysines (~10 %). Post-translational modifications of SLPs can also occur and include addition of glycans, lipids, phosphate or sulfate groups [4,5]; SLP for instance represents one of the first glycoproteins identified in prokaryotes [6].

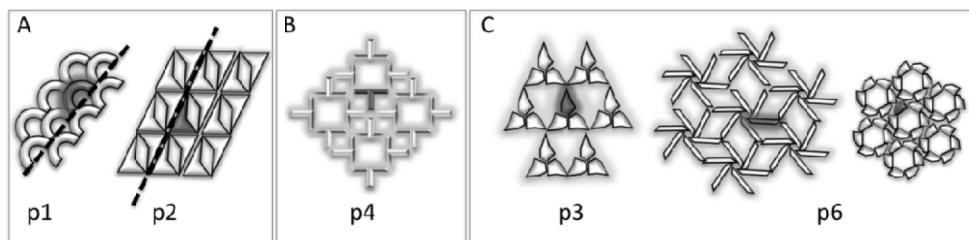


**Fig. 1. Schematic representation of different SLP arrays [3,7,8]**

A. Oblique array; one (p1) or two (p2) identical subunits may adopt the oblique morphological architecture. One individual subunit is shown in grey. B. Tetragonal array (p4) with four subunits. Note that this lattice forms pores of different sizes. C. Hexagonal array that can be composed by three (p3) or six (p6) subunits forming a pinwheel-like structure. In most bacteria, the SLP form oblique or tetragonal lattices, whereas in archaea, the SLP has more frequently a hexagonal symmetry [9].

S-layers exhibit a strong resistance to environmental conditions [10-12], and they protect the cell from stresses such as high temperatures, low pH or high ionic strength. This property is particularly important for extremophiles. Nevertheless, S-layers also serve as an interface between bacterial cell and their environment, forming a meshwork with regularly distributed pores of about 2 to 8 nm to allow nutrient acquisition [13-15]. Some S-layers also allow the passage of proteins with a molecular mass up to 45 kDa, and for this reason they are not a protective barrier against proteases or glycoside hydrolases [16]. These pores, however, play an important role in protein secretion [17]. Several specific functions have been reported for SLPs in cell adhesion or virulence of pathogenic bacteria such as *Clostridium difficile*, *Bacillus anthracis* or *Campylobacter fetus* [18-20]. They can also mediate adhesion of lactobacilli to mammalian epithelial cells, conferring upon these bacteria a protective role in the gastrointestinal tract [21].

Specific protein domains direct the transport of SPLs across the membrane and the anchoring of the protein to the cell surface. Depending on the cell they cover, SLPs are non-covalently attached to either the outer membrane, peptidoglycan or secondary cell wall components (e.g. teichoic acids). In Gram-negative archaea, SLP possesses a hydrophobic anchor associated with the underlying lipid membrane. In Gram-negative eubacteria, SLPs are associated with the lipopolysaccharides mainly via electrostatic interactions [2], whereas in Gram-positive bacteria, S-Layer-like Homology (SLH) motifs have been identified in the amino-terminal region that serve as anchors to the secondary cell wall polymer [22].

As SLPs are always linked to the underlying cell surface through non-covalent forces, they can be easily extracted. Procedures used for extraction may vary, but usually require the use of chaotropic agents such as guanidine hydrochloride for Gram-positive bacteria or metal chelating agents (EDTA) for Gram-negative bacteria [23]. Upon removal of the agent used for isolation, SLPs can be recrystallized to re-form meshworks identical to those on intact bacteria. These new lattices can be formed either in suspension as planar or tube-like structures or on various surfaces including silicon wafers, metal, glass, mica or lipid (Fig. 2 and [24]), a property particularly useful for potential applications in nanobiotechnology [25-27]. Indeed, SLP repetitive building-blocks with a nanometer scale make them very attractive for forming supramolecular scaffolding assemblies. Considering the high density of functional groups on the surface, SLPs are well-defined matrices useful for controlled immobilization of functional molecules such as enzymes, antibodies, antigens, and ligands (as required for affinity and enzyme membranes in the development of solid-phase immunoassays or in biosensors). They may also be used for the formation of inorganic nanocrystal superlattices (e.g. CdS, Au, Ni, Pt, or Pd) as required for molecular electronics and non-linear optics [28].

Considering the use of S-layers as biotemplates for the organization of metal ions or metallic nanoclusters, research on SLP and metals can be understood as an interdisciplinary field, in which different biophysical techniques supply complementary information. In this review, we discuss the potential of SLPs as native or engineered "bottom-up" building blocks for metal immobilization structures. We also describe the biophysical techniques used to analyze metal binding properties as well as the information obtained from the investigation of these structures.

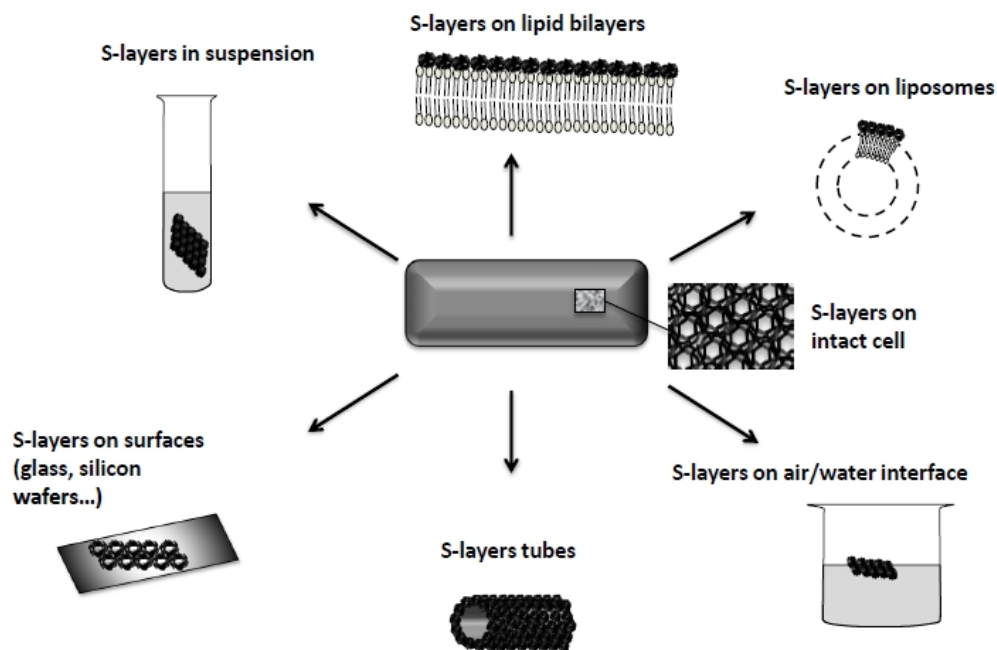
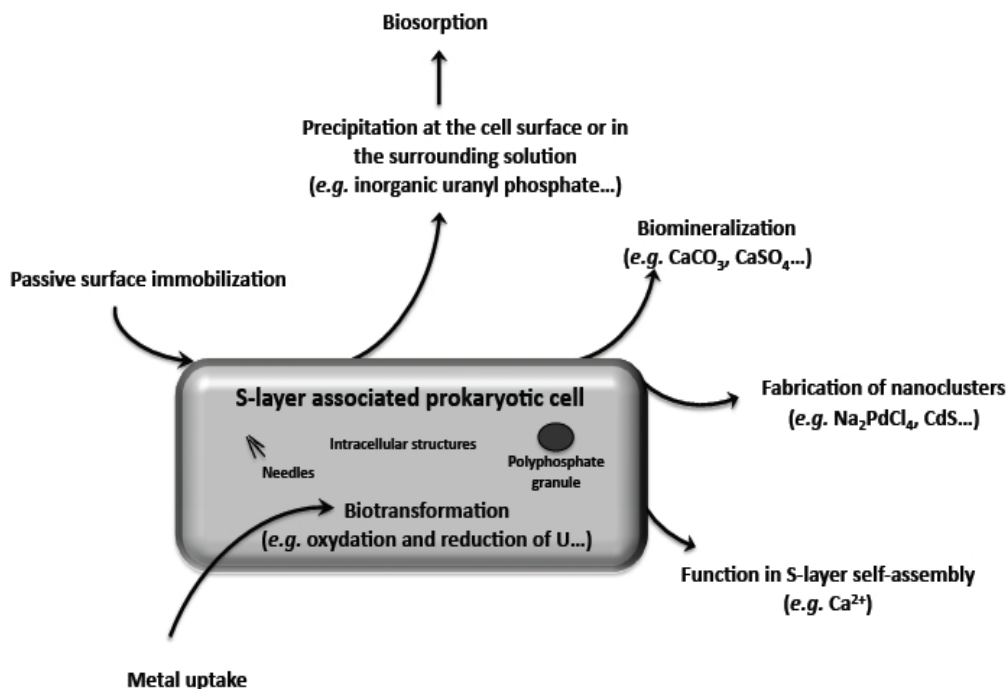


Fig. 2. Schematic representation of SLP assembly in supramolecular structures after recrystallization [27,29]. SLP was not drawn to scale.

## 2. INTERACTION OF SLPS WITH METALS

Prokaryotes are able to survive in extreme conditions, such as hydrothermal wells or waters with high contents of toxic metals; environments not well-tolerated by most eukaryotes. The presence of an S-layer is a common trait in extremophiles and it is considered one special strategy they have developed to survive in these harsh environments. In the case of bacteria that have evolved naturally under chronic exposure to heavy metals [*i.e.*: *Lysinobacillus* (formerly *Bacillus*) *sphaericus* or *Geobacillus* *stearothermophilus*], the capacity to bind and accumulate these metals on the surface of the cell could minimize metal uptake and therefore protect the microorganism from their toxic effects. This ability is of great interest because of its potential use in the removal of metals from contaminated water or soil, as well as for the recovery of precious metals (Au, Pt, Pd, Rh) from industrial wastes. Several genera of microorganisms have been used for such purposes [30-36].

Isolates of *Ly. sphaericus* JG-A12 from a uranium mining waste pile in Germany accumulate high amounts of toxic metals such as U, Cu, Pb, Al, and Cd, as well as precious metals [37]. Among lactic acid bacteria, different species of lactobacilli and bifidobacteria have been successfully used in the removal of Cu, Pb, Cd, Zn and Ni (*Lactobacillus buchneri*, *L. brevis*, *L. kefir*, *L. rhamnosus* GG) [38-40]. In most cases, metal/bacteria interaction was shown to be a fast metabolism-independent surface process, suggesting that binding occurred passively to the surface of bacteria (biosorption) rather than by accumulation inside the cell (bioaccumulation) [38] (Fig. 3). As bacteria often have protein efflux pump systems to prevent metal ion toxicity, storage on the exterior of the cell may thus present a selective advantage with less risk and lower maintenance cost to the cell.



**Fig. 3. Interaction of metals and cells wearing S-layers**

The metal can be passively immobilized by S-layers on the surface of the cell (biosorption) [38,41]. This interaction may also be used as the initial steps to form nanoclusters [42-44]. Metal can also be taken up by bacteria either by an active process using metal transporters or by passive transport due to increased permeability of the membrane under toxic exposure to metal. They can then be bound to undefined cell ultrastructures, form needle-like structures, or associate with polyphosphate granules [45]. Note that uptake is usually limited before cell dies due to metal toxicity. Finally, metal ion immobilization such as in the case of  $\text{Ca}^{2+}$  can be crucial for S-layer assembly [46].

SLPs from different bacteria bind metal ions. SLPs from different strains of *L. kefir* bind  $\text{Pb}^{2+}$ ,  $\text{Cd}^{2+}$ ,  $\text{Zn}^{2+}$  and  $\text{Ni}^{2+}$  [39], and SLPs of *Ly. sphaericus* JG-A12 exhibit a high capacity to bind  $\text{UO}_2^{2+}$  (up to 20 mg U/g protein, [47]) and also bind  $\text{Cu}^{2+}$ ,  $\text{Pd}^{2+}$ ,  $\text{Pt}^{2+}$  and  $\text{Au}^{3+}$  [48,49]. In addition, it is now known that bacteria use horizontal genetic transfer of S-layer encoding genes to propagate their capacity to bind uranium [50]. The capacity of these SLPs to bind selectively and reversibly high amounts of uranium was used to construct a stable porous filter matrix (bioceramic) with a high metal binding capacity, allowing a simple and complete removal of the bound metals, well suited for the reversible usage for bioremediation purposes [37].

As mentioned, isolated SLPs have an intrinsic tendency to self-assemble into two-dimensional arrays in suspension and on various surfaces, exhibiting pores of identical size and morphology and presenting functional groups aligned in a well-defined order and orientation.

These characteristics, together with the possibility of changing their natural properties by genetic manipulation, have attracted great attention because of the potential to generate

specific biomineralization (processes by which organisms form minerals) allowing the construction of defined metal nanoclusters (clusters of particles in a range within 1-100 nm).

SLPs act as templates for cluster formation even in nature (Fig. 3). Indeed, calcium carbonate (calcite) clusters can be formed on the surface of *Synechococcus* cyanobacteria [7]. *Synechococcus* forms a hexagonal S-layer that acts as a template for calcite formation by providing nucleation sites for the mineralization. Mineral formation begins within the holes of the S-layer, where  $\text{Ca}^{2+}$  binds *via* negative charges of the SLP, followed by carbonate binding to initiate the formation of a mineral aggregate. This process depends on the pH and ionic composition of the surrounding solution, so this formation is not restricted to calcite; for example calcium sulfate (gypsum) can also form on SLP [51].

Based on the discovery of mineral formation by SLPs in natural environments, SLPs lattices have been used for patterning of metal ions. The interaction of metal ions with SLPs involves certain functional groups from naturally occurring aminoacid residues, posttranslational modifications of the proteins or modifications introduced through chemical or genetic engineering of the proteins [39,43,52] and these interactions may be used as an initial step in cluster formation. In this sense, the SLP from *Lactobacillus kefir* interacts with metals mainly through coordination with the side chain carboxyl groups of Asp and Glu residues and additional coordinations involving NH groups from the peptide backbone [39]. The SLP from *Ly. sphaericus* interacts with Pd(II) through carboxyl groups [43] while uranium is coordinated to carboxyl groups and to phosphate groups [53]. Phosphate groups are also involved in the interaction of SLP from archaea *Sulfolobus acidocaldarius* DSM 639 with U(VI) [45]. With regard to the engineered SLPs, the introduction of thiol groups, mainly by adding cysteine residues [54] or by chemical modification of aminogroups with iminothiolane [42], was used to achieve a controlled deposition of gold nanoparticles, while the generation of chimeric His<sub>6</sub>-tagged-SLP improved nickel binding capacity of SLP from *Ly. sphaericus* [55,56] and effectiveness in removal of cadmium from water of SLP from *Caulobacter crescentus* [57].

The regular distributed pores of the crystalline arrays offer equivalent spaces for nucleation into nanoclusters of defined size, even if heterogeneity in SLP holes can sometimes be a problem (Fig. 1). For instance, the SLP of *Ly. sphaericus* was used to nucleate gold nanoclusters from thiol groups when exposed to a tetrachloroauric acid solution under electron radiation [42], or to nucleate Pd from carboxyl groups when exposed to a solution of  $\text{Na}_2\text{PdCl}_4$  [43]. The bound Pd(II) can be then reduced to the Pd(0) nanoclusters by the addition of  $\text{H}_2$ , resulting in nanoparticles of 19-43 atoms with a diameter of approximately 1 nm very promising for the development of novel catalysts [37,58]. Similarly, thiol groups of SLPs have been used for the fabrication of CdS nanocrystals of 4-5 nm in size, organized in square symmetry arrays [44].

Bio-nano-Pd supported on Gram negative and Gram positive bacterial types have been successfully used to catalyze the hydrogenation of itaconic acid, giving a yield comparable with commercial 5 % Pd-graphite [59].

The interaction of SLPs with heavy metals has also been used for the construction of metal binding protein based sensors. In this regard, SLPs from *Ly. sphaericus* JG-A12 have been tethered to gold electrodes, to construct a new biosensor responding to picomolar levels of aqueous uranyl ions within minutes [60].

Even as natural SLPs present an attractive tool for metal binding, engineered recombinant SLPs may open a diversity of biological templates for the fabrication of metal nanoclusters. In this regard, the insertion of aminoacid residues carrying functional groups with high affinity for heavy metals may result in a higher efficiency for the metals sequestration. In other words, engineered recombinant SLPs enlarge the possibilities of designing nanoclusters with higher affinity for metals. Direct insertion of cysteine or histidine residues resulted in engineered SLPs with increased metal binding capacity [55]. Moreover, taking into account the available information about the structure of some SLP and the molecular modeling tools, the combination of both also enlarge the possibilities for the engineering SLP with higher affinity for heavy metals. We will turn to this point in section 4.5 (*In silico* structural analysis and molecular modeling).

### 3. APPLICATIONS IN BIOELECTRONICS

According to Willner and Katz, "the basic feature of a bioelectronic device is the immobilization of a biomaterial onto a conductive support, and the electronic transduction of the biological functions associated with the biological matrices" [61].

The application of SLP in bioelectronics must be regarded as an extension of this definition because SLPs themselves have no known functions that can be triggered electronically or electrochemically. In spite of this distinction, the advances in genetic engineering are very promising with regard to the integration of specific functions, such as supramolecular hosts or building blocks of electronic devices on SLPs. Because of the crystalline structure of the S-layer lattices, fused functional sequences that are arranged at well-defined distance and orientation to each other, represent appropriate systems for nanobiotechnological applications [62].

The use of SLP as insulating templates [63] for the synthesis of metal nanoparticles and nanowires offers a simple pathway toward the design of "hybrid bioelectronic devices", combining the advantages of typical supramolecular nanosystems with bioelectronic systems [64]. In these "hybrid systems", S-layers embedded with metal nanoparticles can be used to carry out electrochemical functions, thus mimicking the functions of enzymes (*biomimetics*) [65].

As for bioelectronic applications, net charges are important. It must be emphasized that in general, SLPs by composition are *ca.* 25 % ionic amino acids, which facilitates the electrodeposition of nanoparticles within the SLP structures. This way, SLPs become very suitable biotemplates for binding and subsequent electroreduction of noble metal nanoparticles (*e.g.*: Cu, Ni, Au, Pd, Pt).

In this regard, S-layer nanopores can support either the crystallization of inorganic nanoparticles or their chemical or electrochemical reduction [66]. In addition, the pattern of bound molecules and nanoparticles frequently reflects the lattice symmetry, the size of the morphological units, and the physicochemical properties of the array. This allows several possibilities in the combinations with suitable nanomaterials (*e.g.*: metal, metal oxide or semiconductor particles like  $H[AlCl_4]$ ,  $K_2PtCl_6$ ,  $PdCl_2$ ,  $NiSO_4$ ,  $Cu(SO_4)_2$ ,  $Pb(NO_3)_2$  or  $K_3[Fe(CN)_6]$ ) [67]. The distribution of net negatively charged domains on SLPs could be visualized by electron microscopic methods after labeling with positively charged topographical markers, like the polycation ferritin [68]. Metal (Au) or semiconductor (CdSe) nanoparticles have been either electrostatically or covalently bound onto solid-supported protein monolayers and self-assembly products of SLP from *Ly. sphaericus* CCM 2177 [69].

More recently, an efficient chemical modification of SLPs from *Bacillus subtilis* allowed the anchoring of gold and silver to the protein pores [70]. The introduction of thiol groups has also been used to facilitate the formation of gold nanoparticles from SLPs of *Ly. sphaericus* CCM2177. In addition, S-layers have also been employed as templates for the *in situ* nucleation of ordered two-dimensional arrays of CdS nanocrystals [44]. These results strongly support the fabrication of other inorganic nanocrystal superlattice arrays [42,71].

Nevertheless, the weak point of using a SLP protein to construct an electronic device (a process which requires chemical treatments such as immersion in sulfuric acid or sodium hydroxide) is the stability of the protein. For this reason Presenda et al [72] investigated the window of stability in pH and time of *Deinococcus radiodurans* SLP adsorbed onto platinum surfaces and showed that it retains order over a wide range of pH and after 1000 seconds of exposure to the electrolytes used for the electrochemical fabrication of dense arrays.

The metal binding capacity of SLPs can also be enhanced with the help of molecular biology techniques. In this regard, the addition of his-tags to SLPs improves their Ni-chelating capacity, converting the recombinant proteins into attractive self-assembling biological templates for the fabrication of metal nanoclusters and construction of nanomaterials [55,56,73]. This strategy has also been used for the modification of SLPs from *Caulobacter crescentus*, for the purpose of removing cadmium from water [57].

In the study of SLP/metal interactions a detailed knowledge of a number of structural and functional parameters is of great importance. These structural aspects include the geometry of lattices, the size and distribution of the pores, the secondary and tertiary structure of SLPs and the exact location, orientation and steric accessibility of specific amino acids on the surface and at the protein-protein interfaces. Some of the functional parameters of interest are the magnitude of protein-protein and protein-metal interactions, the chemical groups involved in the coordination of metals, the type of coordination and the structural changes induced in the SLPs and in the S-layers as a result of such interactions. Several different biophysical techniques supplying complementary information can be used for these analyses.

#### **4. METHODS TO ANALYZE THE STRUCTURE OF SLPs AND THEIR INTERACTION WITH METALS**

In the next sections we aim to describe some currently available methods to elucidate the interaction of SLP with metals. To fulfil this aim, the basic information about S-layer and SLP structures is necessary to support the analysis of SLP/metal interaction. For this reason, we first describe elementary methods to analyze basic structures of S-layers and then, how they can be used to characterize further interaction with metals.

##### **4.1 Electron Microscopy**

The regular structure of SLP lattices can be identified by electron microscopy (EM). Various techniques, such as freeze-etching and negative staining, have long been used to characterize SLP meshworks [74,75]. Due to the presence of metal ions, in a fashion similar to that used for negative staining, mineralized SLP from *Synechococcus* have also been directly imaged without the need of further staining [51]. Nevertheless, these two techniques present drawbacks such as the need of sample dehydration and/or staining, which can both alter the geometry of lattices and introduce artifacts. For this reason, the best method now



available to determine S-layer structure is cryo-transmission electron microscopy (cryo-TEM). With this technique, SLPs remain close to their native state as they are rapidly frozen in a hydrated state and observed in the absence of staining and chemical fixation [76] (Fig. 4). In addition, cryoTEM allows to observe the projection of the density of the mass of the object while negative staining just shadows objects. Negative staining thus contains very limited information compared to cryoTEM. Recently, cryo-TEM structures of *G. stearothermophilus* and *Caulobacter crescentus* SLPs have been reported [8,46]. Visualization of S-layers directly on the cell surface of *Caulobacter* have, for instance, provided evidence that lattices are not arranged in a hexagonal pattern over the entire surface of the cell, shown how S-layers grow, and demonstrated areas where SLP newly synthesized patches meet [8]. A combination of cryo-TEM and X-ray crystallography has revealed a new mechanism for SLP assembly, which is triggered by  $\text{Ca}^{2+}$  [46].

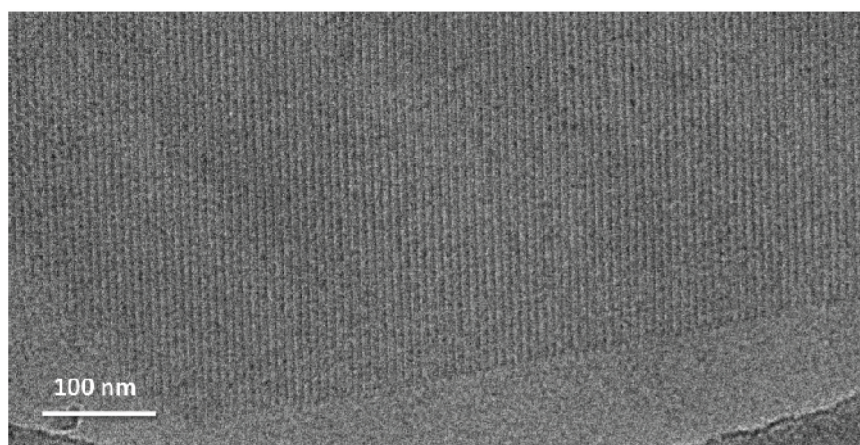


**Fig. 4. Cryo-TEM image of *G. stearothermophilus* SbsB S-layer**

The stripe-like structure corresponds to the SbsB S-layer, the gray area corresponds to the vitrified buffer and darker gray region is the plastic carbon of the grid. Image by the courtesy of R. Fronzes and G. Péhau-Arnaudet (Institut Pasteur, Paris).

Cryo-TEM structures of SLPs bound to metals nanoclusters have not been resolved. However, transmission electron microscopy has been used to observe metal binding. For instance, the interaction of uranium to SLP of *Ly. sphaericus* has been mapped by TEM [77]. Nevertheless, one of the most promising tools is probably the construction of recombinant SLPs allowing the insertion of specific sequences able to bind metal labels [55]. Although only a few genes encoding SLPs have been cloned, the expression or isolation of recombinant proteins clearly opens new possibilities as these tags allow the precise localization of the metal on the SLP lattice by cryo-TEM, thereby providing the opportunity to link the ultrastructure to specific positions in the sequence of SLPs.

Further information will also be given by scanning probe microscopy (atomic force or scanning tunneling microscopy), which give access to useful topographical details of SLPs [11,78].

## 4.2 Atomic Force Microscopy

Atomic Force Microscopy (AFM) has become an important microscopic technique due to its capability to provide three-dimensional topographic views with a high resolution (fractions of

a nanometer). Advantages also include sample preparation since there is no need of staining or protein labeling [79]. Besides imaging, this technique also allows the investigation of intermolecular forces between various ligands and receptor molecules [80,81] and the unfolding forces of individual proteins [82], since it is capable to measure forces of a few piconewtons [83].

A variety of AFM approaches have been developed for investigating surfaces properties, providing novel information on the nanomechanical properties of different surfaces (e.g. microbial cell walls) and the localization of molecular recognition events [84,85]. AFM imaging is particularly useful in the study of biophysical aspects of S-layers including the dynamics and energetics of conformational transformation during folding, self-assembly and recrystallization of SLPs from different kinds of microorganisms [86]. The combined use of AFM imaging and force spectroscopy allowed Müller et al. to investigate the forces holding the individual monomers of SLP from *Deinococcus radiodurans* together, as well as those driving the assembly of the hexameric protomer intermediates (HPI) [87]. In a similar way, Scheuring et al. demonstrated that SLP from *Corynebacterium glutamicum* assembles into hexameric complexes formed by PS2 proteins within a hexagonal lattice [88] (Fig. 5). More recently, S-layer from *G. stearothermophilus* was shown to be a highly stable protein layer able to bear mechanical stress and to change its unfolding pathway because of the binding of a specific ligand such as secondary cell wall polymer [89].

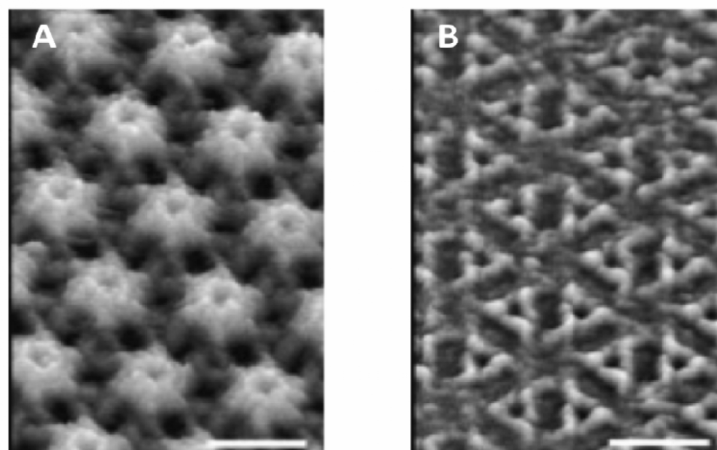


**Fig. 5. High-resolution AFM imaging of S-layer of *Corynebacterium glutamicum* lead to identification of a flower-shaped surface on the cell wall connected side whereas a triangular-shaped surface form on the extracellular surface [taken from ref. 88]**

A. Flower-shaped surface of the native S-layer (scale bar = 15 nm; full grey scale: 3.5 nm).

B. Triangular-shaped surface of the native S-layer (scale bar = 15 nm; full grey scale: 2.0 nm).

As mentioned in the previous section for EM, the possibility of genetically modifying SLP with different functional sequences has enabled the building of a broad range of functionalized nanostructures with defined properties [90]. For example, genetically engineered histidine-tagged CbsA peptides of *Lactobacillus crispatus* were used to study the different molecular forces displayed by their C-terminal and N-terminal regions, which may be biologically relevant in determining CbsA functions [91]. Force spectroscopy was also useful to investigate the topography of the single-molecule array and the functionality of a 2D-crystalline monomolecular protein lattice on a silicon surface generated by SbpA (SLP of *Ly.*

*sphaericus* CCM 2177) carrying the short affinity peptide *Strep*-tag at the C-terminus. This allowed the resolution of structural details of protein alignment and spacing [92,93]. In 2011, Habibi et al. used AFM to imaging the controlled crystallization of IgG functionalized-SLPs from *Bacillus thuringiensis* onto the shell of hollow polyelectrolyte capsules for targeted drug delivery application [94].

AFM has also allowed the study the interactions between SLPs and metal ions [56,95]. Although there are a few reports dealing with this issue, this is an area of particular interest due to the increasing development of nanotechnological applications involving different metals. In particular, Györvary et al. demonstrated that bivalent cations such as calcium ions are not only needed for protein-protein interactions but also for the attachment of proteins to the surface in the recrystallization process of SbpA (SLP from *Ly. sphaericus*) at silicon surfaces [95]. More recently, metal binding properties of the His<sub>6</sub>-tagged SLP SbpA of *Ly. sphaericus* CCM 2177 were investigated by single molecule force microscopy. The His<sub>6</sub>-tag is widely used for specific binding to Ni<sup>2+</sup>-loaded NTA (nitrilotriacetic acid) groups, which were tethered to the AFM tips *via* a flexible polyethylene glycol (PEG) linker. The functionalized tips showed specific interactions with SLP containing His<sub>6</sub>-tags in the presence of nickel ions [56].

### 4.3 X-Ray Crystallography and Small Angle X-Ray Scattering

A significant limitation to obtain structural data for S-layer at an atomic resolution using X-ray crystallography arises from the difficulty in obtaining three-dimensional monocrystals, due to the high propensity of S-layers to form two-dimensional assemblies. Despite that difficulty, crystal structures of truncated and soluble forms of SLPs can be found in the literature. The low-molecular weight component of the *Clostridium difficile* SLP has been solved to 2.4 Å resolution, showing a 2-domain organization [96]. A SAXS envelope could be also obtained showing the interaction between the high- and low-molecular weight components. As SLPs do not belong to a single protein superfamily, the fold observed in the different proteins for which the structure has been solved is very diverse. A 2-layer sandwich architecture has been observed for the N-terminal domain of the *C. difficile* SLP [96], three triple-helix bundles for the N-terminal domain of the SbsC SLP from *G. stearothersophilus* [97], and a β-propeller fold for a putative SLP of the archaeal *Methanosarcina acetivorans* [98] and the Gram-negative bacteria *Bacteroides uniformis* [99]. This technique has also been used to analyze the formation of Pd nanoparticles on crystalline bacterial S-layers, showing the response of the S-layer lattice to the loading with Pd complexes and metallic Pd particles as well as the effects of two different reducing agents (H<sub>2</sub> and dimethylaminoborane) on the nanoparticle arrays [100].

Interestingly, domains displaying a β-propeller fold have homologues in metazoan cell surface proteins, suggesting evolutionary relationships between surface proteins of the three domains of life. In a very recent study, the crystal structure of one of the two homologous tandem polypeptide repeats of the MA0829 S-layer protein of *M. acetivorans* has been determined [101]. Based on the interactions observed in the crystal packing, the authors proposed the first high-resolution model for a microbial SLP. At the same time, another group solved the crystal structure of the SbsB SLP of *G. stearothersophilus* [46]. In this study, the authors combined crystal packing information, chemical crosslinking data and cryo-electron microscopy projections to present a model for the molecular organization of the SbsB S-layer [46]. In addition, this work provided the first structural data at an atomic scale of the role played by Ca<sup>2+</sup> ions in the self-assembly mechanism. Four Ca<sup>2+</sup> ions per monomer are observed stabilizing the interactions between domains (Fig. 6). As these

calcium ions are at key positions for structural transitions important for 2D lattice formation this could explain why calcium binding is so crucial for S-layer assemblies.

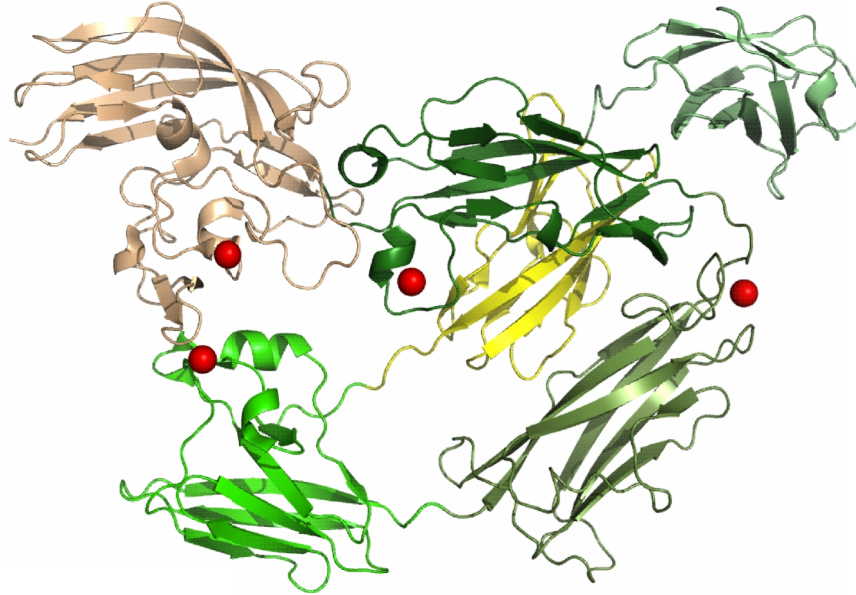


**Fig. 6. Ribbon representation of the structure of one monomer of *G. stearothermophilus* SbsB [46]**

*Ca<sup>2+</sup>* ions are represented by red spheres. SbsB is colored by domains, domain II (residues 202-296) in pale green, domain III (residues 297-388) in yellow, domain IV (residues 389-501) in green, domain V (residues 502-630) in light green, domain VI (residues 631-739) in forest green, and domain VII (residues 740-920) in wheat.

#### **4.4 *In silico* Structural Analysis and Molecular Modeling**

One of the main limitations to understanding some of the functions of microbial SLPs comes from the lack of knowledge regarding their three-dimensional organization. A three-dimensional structural analysis of SLPs usually poses some difficulties resulting from the following: *i*) the molecular mass of the SLP subunits is too large for structural studies by nuclear magnetic resonance (NMR); *ii*) SLPs in solution form crystallized monomolecular layers rather than isotropic three dimensional crystals, making three dimensional experimental studies by X-ray crystallography problematic. The dissolved proteins immediately interact to form small oligomers, which provide the nucleation seed for the formation of large layers. Furthermore, some SLPs do not fold into their native tertiary structure as monomers in solution, but rather condense into amorphous clusters in an extended conformation. Only when assembled into the lattice structure, are they able to restructure into their native conformation.

The experimental structural analysis problems resulting from biochemical properties of the SLPs can be overcome using molecular modeling, which appears to provide an appropriate tool to examine in atomic detail the dynamics and structure-function relationships of the tridimensional organization of SLPs.

Considering the wide range of applications of SLPs, clarifying the tertiary structure, and therefore, the exact distribution of the amino acids in the lattices becomes very important. The main goals of molecular modeling applied to proteins are: *i)* to predict the native structure of a protein from its sequence; *ii)* to refine the structure of a protein from the experimental data; *iii)* to generate the conformations of a protein during the folding or unfolding process; *iv)* to predict interaction of proteins with metals [102,103].

In regard to SLPs, it must be underlined that taking into account that working with these proteins is somehow difficult from an experimental point of view, *in silico* results may give relevant information about their architecture and the changes induced by heavy metals. However, up to our knowledge only Horejs et al. [104,105] combined SLPs with molecular modeling.

As for the analysis of other proteins, the modeling of the tertiary structure of SLPs usually begins with an analysis of the amino acid sequence. With this information, a sequence homology searching aids in the identification of the conserved motifs with relevance from the structural or functional point of view. All this information contributes to the successful determination of the tertiary structure of SLPs, including free energy and other physicochemical parameters.

The first structural model of an SLP at atomic resolution was reported in 2008 [104]. In that work, the tertiary structure of the SLP of *G. stearothermophilus* PV72/p2 was predicted from the amino acid sequence. In addition, these authors could model the lattice itself from the consideration of some characteristics, such as pores, size and functionalization.

More recently, the self-assembly processes of SLPs in solution were investigated theoretically using a Monte Carlo approach [105]. In that work, C. Horejs et al. determined that only few and mainly hydrophobic amino acids on the surface of the monomer are responsible for the formation of a highly ordered anisotropic protein lattice. They were able to accurately reproduce many experimentally observed features including pore formation, a chemical description of the pore structure, location of specific amino acid residues at the protein-protein interfaces, and the surface accessibility of specific amino acid residues.

Even though the investigation of SLPs using modeling tools is very recent, it represents a field where researchers may find several answers that are difficult to elucidate from an experimental point of view. In this regard, *in silico* based methods offer an invaluable tool to capture details of primary sequences and to explore morphological structures with thousands of protein monomers, to spread design rules for the spontaneous formation of specific protein assemblies.

The relevance of S-layer proteins as patterning elements in life and non-life sciences highlights the relevance of these works. Furthermore, Horejs et al. consider that a deeper insight on the location, orientation, and steric accessibility of the SLP binding sites is crucial for the development of other applications of SLPs, including the precipitation of metal ions from solutions [104]. Even when the authors recognize the importance of investigations directed toward the analysis of S-layer binding sites, information about modeling of SLPs is scarce, representing a domain where much work remains to be done.

#### **4.5 X-Ray Absorption Spectroscopy**

X-ray absorption spectroscopy (XAS) is a non-destructive method allowing the determination

of local coordination environments of specific elements such as metals. Because of its ability to examine samples under *in situ* conditions with minimal preparation, XAS spectroscopy has become the most important method for determining the speciation of uranium, zinc, lead and arsenic, which are often present in complex, multiphase, natural samples at concentrations ranging from greater than a weight percent to less than a ppm in a variety of chemical forms [106]. In particular, XAS has been used for determining the complexes formed between SLPs and environmental pollutants such as uranium, zinc, lead or arsenic. Extended X-ray Absorption Fine Structure (EXAFS) analyses demonstrated that in *Ly. sphaericus* SLP, uranium is coordinated to carboxyl groups in a bidentate way with an average distance between the uranium and the carbon atom of 2.88 Å and to phosphate groups in a monodentate way with an average distance between the uranium and the phosphorus atom of 3.62 Å [53].

X-ray absorption fine structure (XANES) provides the most direct experimental information about the occupied and unoccupied electronic states of a given template. Therefore, this spectroscopic technique was used to characterize electronic properties of SLPs from *Ly. sphaericus* NCTC 9602, widely used as template for the bottom-up fabrication of advanced metallic and hybrid nanostructures. The results obtained showed that the  $\pi$  clouds of aromatic rings make the main contribution to both the lowest unoccupied and highest occupied molecular orbitals. The two-dimensional protein crystal shows a semiconductor-like behaviour with a gap value of  $\sim 3.0$  eV and the Fermi energy close to the bottom of the LUMO [107].

#### 4.6 Time Resolved Induced Laser Fluorescence Spectroscopy

Time resolved induced laser fluorescence spectroscopy (TRLFS) allows the study of the complex formation of actinides (*e.g.* uranium, americium, and curium) and lanthanides (*e.g.* europium). TRLFS is a very sensitive method which can give insights on complex formation and provide information on the interaction of metal ions with bacteria SLPs. It is based on the fact that the measured fluorescence lifetime and intensity of the electronic transition of the excited metal ions are dependent on their molecular environment and the information obtained from this method is complementary to that obtained with XAS [53,108,109]. Reitz carried out TRLF spectroscopic analyses on bacterial and archaeal samples, grown and treated with U (VI) [45]. The author evaluated the influence of aeration conditions and the effect of pH on the metal complex formation with bacterial organic molecules demonstrating that besides the phosphate groups of the cell membrane, deprotonated carboxylic groups are involved in the U (VI) complexation by the cells of the acidothermophilic archaea *Sulfolobus acidocaldarius* at pH 4.5. In this regard, TRLFS and EXAFS showed that the accumulated U (VI) was complexed mainly through organic phosphate groups in the S-layer of *Sulfolobus acidocaldarius* DSM 639 [45].

#### 4.7 Quartz Crystal Microbalance and Surface Plasmon Resonance

Quartz crystal microbalance (QCM) and Surface Plasmon Resonance (SPR) are two label-free surface-sensitive techniques used to follow SLP self-assembly on solid surfaces in real time. These methodologies involve an ultrasensitive mass sensor that monitors real time changes in the adsorbed amount of material. They allow the investigation of the mechanisms of recrystallization of SLPs at a nanoscale level and therefore it is important for understanding and engineering of biomembranes and biosensors [110]. QCM has for instance been used to follow *in situ* the self-assembly of SLPs from solution to solid

substrates on gold or SiO<sub>2</sub> surfaces [111] and also used to investigate *in situ* the electrochemical behavior of the SLPs on gold electrodes with the capability to measure mass changes at the nanogram level at the electrode surface/electrolyte interfaces [94,112,113].

#### 4.8 Neutron Reflectometry

Neutron Reflectometry (NR) has emerged as a powerful tool for the investigation of polymer surfaces as it provides good spatial resolution (~ 1 nm) with penetration depths over hundreds of nanometers. As NR allows the detection of variations in thickness (that can be estimated from the spacing of the minima of two neighboring interference fringes) and roughness of the S-layer, it can be particularly useful to analyze S-layers after recrystallization. Indeed, NR was used to show that recrystallized SLP builds loosely packed layers, which incorporate around 68 % water [114]. As NR can also be used to analyze the interface between underlying material and metals [115], the technique also provides support for analyzing SLP self-assembly and interaction with metals.

#### 4.9 Fourier Transform Infrared Spectroscopy

The structural analysis of SLPs provides support for the development of nanotechnological applications. The secondary structure of SLPs has been determined using circular dichroism measurements, FTIR spectroscopy and especially, the prediction based on the available protein sequence data [116]. No common patterns can be established. For some microorganisms, the secondary structure is dominated by  $\alpha$ -helices [117] whereas for others  $\beta$ -sheets account for ca. 40 % of the secondary structures [118]. In addition, the secondary structure of SLPs has been related with some superficial properties of the whole microorganism, like aggregation. In this sense, the SLPs from non-aggregative lactobacilli have higher  $\beta$ -sheet contents than those from aggregative strains. These results suggest that the secondary structures of SLP of analyzed lactobacilli play an important role in determining the surface properties of whole bacteria [118].

The interaction of SLPs with metals has also been addressed using FTIR. Fahmy et al. have characterized the interaction SLP/Pd in *Ly. sphaericus* [43]. These authors reported the crucial role of carboxyl groups in binding Pd(II), and in the stabilization of SLP in the complex. More recently, this group revealed by FTIR the impact of Au-nanocluster formation on protein structure and stability, hypothesizing that Au-nanoclusters expel water from protein cavities resulting in an increased local hydrophobicity which destabilizes the negative charge of side chain carboxylates. They conclude that the SLPs provide a biotemplate for efficient Au-nanocluster formation. Cluster growth distorts the protein secondary structure, but *vice versa*, the protein matrix is rigid enough to restrict cluster growth to about 2 nm particle size. The resulting Au-nanoparticle-loaded S-layer exhibits a high stability against acid denaturation [119].

Among lactic acid bacteria, the relation between SLPs and metal sequestration has also been addressed. *L. kefir* strains (CIDCA 8348 and JCM 5818) are for instance efficient in the removal of Pb, Cd and Zn and accurate and quantitative models based on a FTIR related methodology (Raman spectroscopy) and multivariate analysis have been used for the quantification of these metals when adsorbed to the bacterial surface [120].

The interaction of pure SLPs with metal ions induces important changes in protein structure. Indeed, the SLP/metal interaction occurs mainly through coordination with the side chain carboxylate groups of the Asp and Glu residues. This coordination is predominantly unidentate and is complemented by additional coordinations involving NH groups from the peptide backbone. In addition, the interaction with metals also induces changes in the secondary structure of the SLPs. These changes obey a general trend of increasing the amount of  $\beta$ -sheet structures and reducing the  $\alpha$ -helices, which allows the proteins to adjust their structure to the presence of the metal ions at minimum energy expense (Fig. 7). Accordingly, as a trend, larger ions produced more significant changes in the secondary structure of the studied proteins [39].

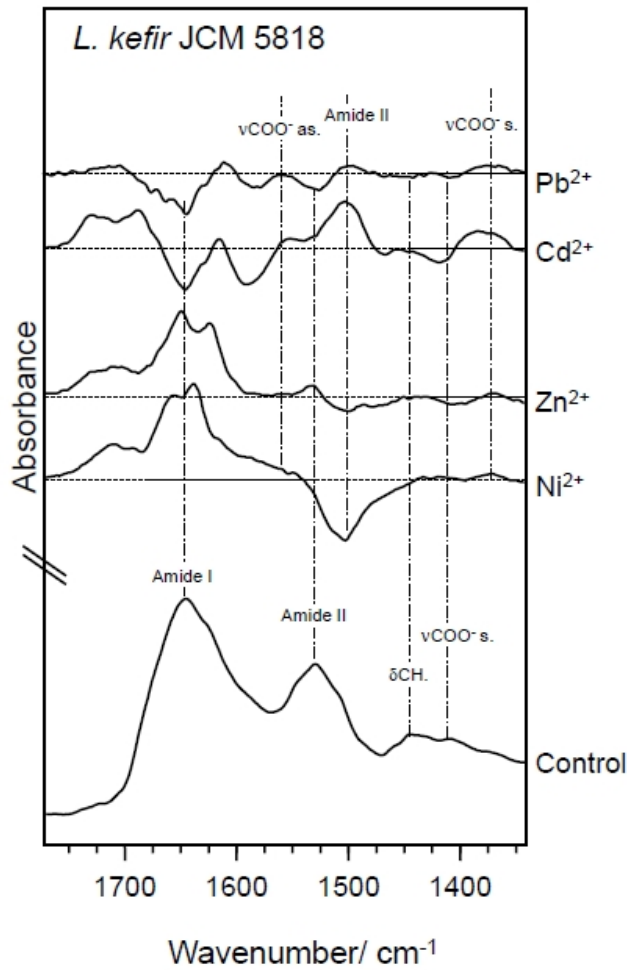


**Fig. 7. FTIR difference spectra of S-layer proteins from strain *L. kefir* JCM 5818 induced by  $\text{Ni}^{2+}$ ,  $\text{Zn}^{2+}$ ,  $\text{Cd}^{2+}$  and  $\text{Pb}^{2+}$  binding**  
*Control: FTIR spectrum of non-treated SLP. In obtaining the difference spectra, the original spectra were normalized to the  $\delta\text{CH}$  internal standard. Dashed horizontal lines define the zero of the ordinate scale of the difference spectra [39].*



## 5. CONCLUSIONS

Isolated S-layer proteins have the natural tendency to reassemble in suspension and on various surfaces into two-dimensional monomolecular arrays with pores and functional groups regularly distributed down to the nanometer scale. These characteristics have attracted attention for their numerous potential applications as building blocks in nanobiotechnology and biomimetics.

Furthermore, the strain-dependent metal binding abilities of some S-layers make them interesting for technical applications in bioremediation, construction of bioelectronic devices and catalysis. These abilities can be enhanced through genetic manipulation in a way where functionalized S-layer proteins still maintain their ability to recrystallize, leading to the generation of new affinity matrices, biosensors or specific metallic nanoclusters at surfaces. From basic and applied research, a number of methodologies have arisen that allow a detailed study of the structure, morphology, physical chemistry and function of native and engineered SLPs, alone or in presence of different ligands.

As has been the case for several millions of years, bacteria and archea have their S-layers assembled and ready to work. Now is our turn to find a job for them to do.

## ACKNOWLEDGEMENTS

The authors acknowledge the financial support of ECOS-Sud program (A09B02), Argentinean Agency for the Promotion of Science and Technology (Projects PICT/2011/0226; PICT/2010/2361), Argentinean National Research Council (CONICET) (Project PIP 114-201101-00024), University Paris Diderot, CNRS and CEA. P.M., M.S. and A.G.-Z. are members of the research career CONICET. We are grateful to G. Pehau-Arnaudet and S. Marco for fruitful discussion, to R.R. Sinden (South Dakota School of Mines and Technology, USA) and R.A. Lease (Ohio State University, USA) for critically reading this manuscript.

## COMPETING INTERESTS

The authors declare that they have no competing interests.

## REFERENCES

1. Calabi E, Ward S, Wren B, Paxton T, Panico M, Morris H, Dell A, Dougan G, Fairweather N. Molecular characterization of the surface layer proteins from *Clostridium difficile*. Mol. Microbiol. 2001;40:1187-99.
2. Avall-Jaaskelainen S, Palva A. *Lactobacillus* surface layers and their applications. FEMS Microbiol Rev. 2005;29:511-29.
3. Sleytr UB, Egelseer EM, Ilk N, Pum D, Schuster B. S-Layers as a basic building block in a molecular construction kit. FEBS J. 2007;274:323-34.
4. Boot HJ, Pouwels PH. Expression, secretion and antigenic variation of bacterial S-layer proteins. Mol Microbiol. 1996;21:1117-23.
5. Konrad Z, Eichler J. Lipid modification of proteins in Archaea: attachment of a mevalonic acid-based lipid moiety to the surface-layer glycoprotein of *Haloflex volcanii* follows protein translocation. Biochem J. 2002;366:959-64.

6. Mescher MF, Strominger JL. Purification and characterization of a prokaryotic glucoprotein from the cell envelope of *Halobacterium salinarium*. J Biol Chem. 1976;251:2005-14.
7. Schultze-Lam S, Harauz G, Beveridge TJ. Participation of a cyanobacterial S layer in fine-grain mineral formation. J Bacteriol. 1992;174:7971-81.
8. Amat F, Comolli LR, Nomellini JF, Moussavi F, Downing KH, Smit J, Horowitz M. Analysis of the intact surface layer of *Caulobacter crescentus* by cryo-electron tomography. J Bacteriol. 2010;192:5855-65.
9. Messner P, Sleytr UB. Crystalline bacterial cell-surface layers. Adv Microb Physiol. 1992;33:213-75.
10. Toca-Herrera JL, Moreno-Flores S, Friedmann J, Pum D, Sleytr UB. Chemical and thermal denaturation of crystalline bacterial S-layer proteins: an atomic force microscopy study. Microsc Res Tech. 2004;65:226-34.
11. Martin-Molina A, Moreno-Flores S, Perez E, Pum D, Sleytr UB, Toca-Herrera JL. Structure, surface interactions, and compressibility of bacterial S-layers through scanning force microscopy and the surface force apparatus. Biophys J. 2006;90:1821-29.
12. Delcea M, Krastev R, Gutlebert T, Pum D, Sleytr UB, Toca-Herrera JL. Mapping bacterial surface layers affinity to polyelectrolytes through the building of hybrid macromolecular structures. J Nanosci Nanotechnol. 2007;7:4260-66.
13. Hovmoller S, Sjogren A, Neng Wang D. The structure of crystalline bacterial surface layers. Prog Biophys Mol Biol. 2008;51:131-63.
14. Sara M, Pum D, Sleytr UB. Permeability and charge-dependent adsorption properties of the S-layer lattice from *Bacillus coagulans* E38-66. J Bacteriol. 1992;174:3487-93.
15. Sleytr UB, Beveridge TJ. Bacterial S-layers. Trends Microbiol. 1999;7:253-60.
16. Sleytr UB, Messner P. Crystalline surface layers on bacteria. Annu Rev Microbiol. 1983;37:311-39.
17. Sara M, Sleytr UB. Molecular sieving through S layers of *Bacillus stearothermophilus* strains. J Bacteriol. 1987;169:4092-98.
18. Grogono-Thomas R, Dworkin J, Blaser MJ, Newell DG. Roles of the surface layer proteins of *Campylobacter fetus* subsp. *fetus* in ovine abortion. Infect Immun. 2000;68:1687-91.
19. Calabi E, Fairweather N. Patterns of sequence conservation in the S-Layer proteins and related sequences in *Clostridium difficile*. J Bacteriol. 2002;184:3886-97.
20. Kern J, Schneewind O. BslA, the S-layer adhesin of *B. anthracis*, is a virulence factor for anthrax pathogenesis. Mol Microbiol 2010;75:324-32.
21. Frece J, Kos B, Svetec IK, Zgaga Z, Mrsa V, Susković J. Importance of S-layer proteins in probiotic activity of *Lactobacillus acidophilus* M92. J Appl Microbiol. 2005;98:285-92.
22. Sara M, Sleytr UB. S-Layer proteins. J Bacteriol. 2000;182:859-68.
23. Sidhu MS, Olsen I. S-layers of *Bacillus* species. Microbiology. 1997;143:1039-52.
24. Bobeth M, Blecha A, Blüher A, Mertig M, Korkmaz N, Ostermann K, Rödel G, Pompe W. Formation of tubes during self-assembly of bacterial surface layers. Langmuir. 2011;27:15102-11.
25. Jaenicke R, Welsch R, Sara M, Sleytr UB. Stability and self-assembly of the S-layer protein of the cell wall of *Bacillus stearothermophilus*. Biol Chem Hoppe Seyler. 1985;366:663-70.
26. Sara M, Sleytr UB. Crystalline bacterial cell surface layers (S-layers): from cell structure to biomimetics. Prog Biophys Mol Biol. 1996;65:83-111.

27. Poppinga L, Janesch B, Fünfhaus A, Sekot G, Garcia-Gonzalez E, Hertlein G, et al. Identification and functional analysis of the S-layer protein SplA of *Paenibacillus larvae*, the causative agent of American Foulbrood of honey bees. *PLoS Pathog.* 2012;8(5):e1002716.
28. Sleytr UB, Bayley H, Sára M, Breitwieser A, Küpcü S, Mader C, et al. Applications of S-layers. *FEMS Microbiol Rev.* 1997;20:151-75.
29. Toca-Herrera JL, Krastev R, Bosio V, Küpcü S, Pum D, Fery A, et al. Recrystallization of bacterial S-layers on flat polyelectrolyte surfaces and hollow polyelectrolyte capsules. *Small.* 2005;1:339-48.
30. Ahluwalia SS, Goyal D. Microbial and plant derived biomass for removal of heavy metals from wastewater. *Bioresour Technol.* 2007;98:2243-57.
31. Barkay T, Schaefe J. Metal and radionuclide bioremediation: issues, considerations and potentials. *Curr Opin Microbiol.* 2001;4:318-23.
32. Cayllahua JEB, de Carvalho RJ, Torem ML. Evaluation of equilibrium, kinetic and thermodynamic parameters for biosorption of nickel(II) ions onto bacteria strain *Rhodococcus opacus*. *Miner Eng.* 2009;22:1318-25.
33. Iwamoto T, Nasu M. Current bioremediation practice and perspective. *Biosci Bioeng.* 2001;92:1-8.
34. Kretschmer XC, Meitzner G, Gardea-Torresdey JL, Webb R. Determination of Cu environments in the *Cyanobacterium anabaena flos-aquae* by X-Ray Absorption Spectroscopy. *Appl Environ Microbiol.* 2004;70:771-80.
35. Selenska-Pobell S, Panak P, Miteva V, Bernhard G, Nitsche H. Selective accumulation of heavy metals by three indigenous *Bacillus* strains, *B. cereus*, *B. megaterium* and *B. sphaericus*, from drain waters of a uranium waste pile. *FEMS Microbiol Ecol.* 1999;29:59-67.
36. Valls M, de Lorenzo V. Exploiting the genetic and biochemical capacities of bacteria for the remediation of heavy metal pollution. *FEMS Microbiol Rev.* 2002;26:327-38.
37. Pollmann K, Raff J, Merroun M, Fahmy K, Selenska-Pobell S. Metal binding by bacteria from uranium mining waste piles and its technological applications. *Biotechnol Adv.* 2006;24:58-68.
38. Halttunen T, Salminen S, Tahvonen R. Rapid removal of lead and cadmium from water by specific lactic acid bacteria. *Int J Food Microbiol.* 2007;114:30-35.
39. Gerbino E, Mobili P, Tymczynsyn E, Fausto R, Gómez-Zavaglia A. FTIR spectroscopy structural analysis of the interaction between *Lactobacillus kefir* S-layers and metal ions. *J Molec Struct.* 2011;987:186-92.
40. Schut S, Zauner S, Hampel G, König H, Claus H. Biosorption of copper by wine-relevant lactobacilli. *Int J Food Microbiol.* 2011;145:126-31.
41. Allievi MC, Sabbione F, Prado-Acosta M, Palomino MM, Ruzal SM, Sanchez-Rivas C. Metal biosorption by surface-layer proteins from *Bacillus* species. *J Microbiol Biotechnol* 2011;21(2):147-53.
42. Dieluweit S, Pum D, Sleytr UB. Formation of a gold superlattice on an S-layer with square lattice symmetry. *Supramolecular Science.* 1998;5:15-9.
43. Fahmy K, Merroun M, Pollmann K, Raff J, Savchuk O. Secondary structure and Pd(II) coordination in S-layer proteins from *Bacillus sphaericus* studied by infrared and X-ray absorption spectroscopy. *Biophys J.* 2006;91:996-1007.
44. Shenton W, Pum D, Sleytr UB, Mann S. Synthesis of cadmium sulphide superlattices using self-assembled bacterial S-layers. *Nature.* 1997;389:585-87.
45. Reitz, T. (2011). U(VI) bioaccumulation by *Paenibacillus* sp. JG-TB8 and *Sulfolobus acidocaldarius*; Au(0) nanoclusters formation on the S-layer of *S. acidocaldarius*. Fakultät für Chemie und Physik der Technischen Freiberg, Universität Bergakademie Freiberg genehmigte. Doctor rerum naturalium.

46. Baranova E, Fronzes R, Garcia-Pino A, Van Gerven N, Papapostolou D, Péhau-Arnaudet G et al. SbsB structure and lattice reconstruction unveiled  $\text{Ca}^{2+}$  triggered SLP assembly. *Nature*. 2012;487:119-24.
47. Raff J. Wechselwirkungen der Hüllproteine von Bakterien aus Uranabfallhalden mit Schwermetallen, PhD thesis. Forschungszentrum Rossendorf, Dresden. German; 2002.
48. Soltmann U, Raff J, Selenska-Pobell S, Matys S, Pompe W, Böttcher W. Biosorption of heavy metals by sol-gel immobilized *Bacillus sphaericus* cells, spores and S-layers. *J Sol-Gel Sci Techn*. 2003;26:1209-12.
49. Raff J, Soltmann U, Matys S, Selenska-Pobell S, Böttcher H, Pompe W. Biosorption of uranium and copper by biocers. *Chem Mat*. 2003;15:240-44.
50. Pollmann K, Raff J, Schnorpfeil M, Radeva G, Selenska-Pobell S. Novel surface layer protein genes in *Bacillus sphaericus* associated with unusual insertion elements. *Microbiology*. 2005;151(Pt 9):2961-73.
51. Schultze-Lam S, Beveridge TJ. Nucleation of celestite and strontianite on a cyanobacterial S-layer. *Appl Environ Microbiol*. 1994;60:447-53.
52. Kinns H, Howorka S. The surface location of individual residues in a bacterial S-layer protein. *J Mol Biol*. 2008;377:589-604.
53. Merroun ML. Interactions between metals and bacteria: Fundamental and Applied Research. In: A. Méndez-Vilas editor. *Communicating Current Research and Educational Topics and Trends in Applied Microbiology* Formatex, Badajoz, Spain; 2007.
54. Badelt-Lichtblau H, Kainz B, Völlenkne C, Egelseer EM, Sleytr UB, Pum D et al. Genetic engineering of the S-layer protein SbpA of *Lysinibacillus sphaericus* CCM 2177 for the generation of functionalized nanoarrays; *Bioconjug Chem*. 2009;20:895-903.
55. Pollmann K, Matys S. Construction of an S-layer protein exhibiting modified self-assembling properties and enhanced metal binding capacities. *Appl Microbiol and Biotechnol*. 2007;75:1079-85.
56. Tang J, Ebner A, Kraxberger B, Leitner M, Hykollari A, Kepplinger C, Grunwald C et al. Detection of metal binding sites on functional S-layer nanoarrays using single molecule force spectroscopy. *J Struct Biol*. 2009;168:217-22.
57. Patel J, Wilson G, McKay RM, Vincent R, Xu Z. Self-immobilization of recombinant *Caulobacter crescentus* and its application in removal of cadmium from water. *Appl Biochem Biotechnol*. 2010;162:1160-73.
58. Wahl R, Mertig M, Raff J, Selenska-Pobell S, Pompe W. Electron-beam induced formation of highly ordered palladium and platinum nanoparticle arrays on the S layer of *Bacillus sphaericus* NCTC 9602. *Adv Mater*. 2001;13:736-40.
59. Creamer NJ, Mikheenko IP, Yong P, Deplanche K, Sanyahumbi D, Wood J, et al. Novel supported Pd hydrogenation bionanocatalyst for hybrid homogeneous/heterogeneous catalysis. *Catal Today*. 2007;128:80-87.
60. Conroy DJR, Millner PA, Stewart DI and Pollmann K. Biosensing for the Environment and Defence: Aqueous Uranyl Detection Using Bacterial Surface Layer Proteins. *Sensors*. 2010;10:4739-55.
61. Willner I, Katz E. Integration of layered redox proteins and conductive supports for bioelectronic applications. *Angew Chem Int Ed*. 2000;39:1180-218.
62. Pleschberger M, Neubauer A, Egelseer EM, Weigert S, Lindner B, Sleytr UB, et al. Generation of a functional monomolecular protein lattice consisting of an S-layer fusion protein comprising the variable domain of a camel heavy chain antibody. *Bioconjugate Chem*. 2003;14:440-8.

63. Huczko A. Template-based synthesis of nanomaterials. *Appl Phys A: Mater Sci Process*. 2000;70:365-76.
64. Mark SS, Bergkvist M, Yang X, Angert ER, Batt CA. Self-assembly of dendrimer-encapsulated nanoparticle arrays using 2-D microbial S-layer protein biotemplates. *Biomacromolecules*. 2006;7:1884-97
65. Espand R, Tomalia DA. Poly (amidoamine) (PAMAM) dendrimers: from biomimicry to drug delivery and biomedical applications. *Drug Discovery Today*. 2001;6:427-36.
66. Schuster B, Sleytr UB. S-layer-supported lipid membranes. *Rev Mol Biotechnol*. 2000;74:233-54.
67. Willner I, Katz E. S-layer proteins in bioelectronic applications. In: Bossmann SH editor. *Bioelectronics: from Theory to Applications*. New York. Wiley; 2005.
68. Sleytr UB, Sára M, Pum D, Schuster B. Molecular nanotechnology and nanobiotechnology with two-dimensional protein crystals (S-layers). In: Rosoff M. editor. *Nano-surface chemistry*. New York, Basel: Marcel Dekker, Inc; 2001.
69. Györfvay E, Schroedter A, Talapin DV, Weller H, Pum D, Sleytr UB. Formation of nanoparticle arrays on S-layer protein lattices. *J Nanosci Nanotechnol*. 2004;4:115-20.
70. Puranik SS, Joshi HM, Ogale SB, Paknikar KM. Hydrazine based facile synthesis and ordered assembly of metal nanoparticles (Au, Ag) on a bacterial surface layer protein template. *J Nanosci Nanotechnol*. 2008;8:3565-69.
71. Sleytr UB, Györfvay E, Pum D. Crystallization of S-layer protein lattices on surfaces and interfaces. *Progress in Organic Coatings*. 2003;47:279-87.
72. Presenda A, Allred DB, Baneyx F, Schwartz DT, Sarikaya M. Stability of S-layer proteins for electrochemical nanofabrication. *Colloid Surface B*. 2007;57:256-61.
73. Korkmaz N, Börrnert F, Köhler D, Mendes RG, Bachmatiuk A, Rummeli MH et al. Metallization and investigation of electrical properties of *in vitro* recrystallized mSbsC-eGFP assemblies. *Nanotechnology*. 2011;22:375606-14.
74. Messner P, Pum D, Sára M, Stetter KO, Sleytr UB. Ultrastructure of the cell envelope of the archaeobacteria *Thermoproteus tenax* and *Thermoproteus neutrophilus*. *J Bacteriol*. 1986;166:1046-54.
75. Smit J, Engelhardt H, Volker S, Smith SH, Baumeister W. The S-layer of *Caulobacter crescentus*: three-dimensional image reconstruction and structure analysis by electron microscopy. *J Bacteriol*. 1992;174:6527-38.
76. Dubochet J, Adrian M, Chang JJ, Homo JC, Lepault J, McDowell AW et al. Cryo-electron microscopy of vitrified specimens. *Q Rev Biophys*. 1988;21:129-228.
77. Merroun ML, Raff J, Rossberg A. Complexation of uranium by cells and S-layer sheets of *Bacillus sphaericus* JG-A12. *Appl Environ Microbiol*. 2005;71:5532-43.
78. Firtel M, Beveridge TJ. Scanning probe microscopy in microbiology. *Micron*. 1995;26:347-62.
79. Dorobantu L, Goss G, Burrell R. Atomic force microscopy: A nanoscopic view of microbial cell surfaces. *Micron*. 2012;43:1312-22.
80. Ebner A, Wildling L, Kamruzzahan AS, Rankl C, Wruss J, Hahn CD et al. A new, simple method for linking of antibodies to atomic force microscopy tips. *Bioconjugate Chem*. 2007;18:1176-84.
81. Hinterdorfer P, Dufrene YF. Detection and localization of single molecular recognition events using atomic force microscopy. *Nature Methods*. 2006;3:347-55.
82. Bornschlögl T, Rief M. Single-molecule protein unfolding and refolding using stomic force microscopy. *Methods in Molecular Biology*. In: Peterman and Wuite editors. *Single Molecules Analysis*. 2011;783:233-50.
83. Fisher TE, Marszalek PE, Oberhauser AF, Carrion-Vázquez M, Fernández JM. The micromechanics of single molecules studied with atomic force microscopy. *J Physiol*. 1999;520:5-14.

84. Gaboriaud F, Dufrêne YF. Atomic force microscopy of microbial cells: application to nanomechanical properties, surface forces and molecular recognition forces. *Colloid Surface B*. 2007;54:10-9.
85. Francius G, Alsteens D, Dupres V, Lebeer S, De Keersmaecker S, Vanderleyden J, Dufrêne YF. Stretching polysaccharides on live cells using single molecule force spectroscopy. *Nature Protocols*. 2009;4:939-46.
86. Shin S, Chung S, Sanii B, Comolli LR, Bertozzi CR, De Yoreo JJ. Direct observation of kinetic traps associated with structural transformations leading to multiple pathways of S-layer assembly. *Proc Natl Acad Sci USA*. 2012;109:12968-73.
87. Müller DJ, Baumeister W, Engel, A. Controlled unzipping of a bacterial surface layer with atomic force microscopy. *Proc Natl Acad Sci USA*. 1999;96:13170-4.
88. Scheuring S, Stahlberg H, Chami M, Houssin C, Rigaud JL, Engel A. Charting and unzipping the surface layer of *Corynebacterium glutamicum* with the atomic force microscopy. *Mol Microbiol*. 2002;44:675-84.
89. Horejs C, Ristl R, Tscheliessnig R, Sleytr UB, Pum D. Single-molecule force spectroscopy reveals the individual mechanical unfolding pathways of a surface layer protein. *J Biol Chem*. 2011;286:27416-24.
90. Sleytr UB, Huber C, Ilk N, Pum D, Schuster B, Egelseer EM. S-layers as a tool kit for nanotechnological applications. *FEMS Microbiol Lett*. 2007;267:131-44.
91. Verbelen C, Antikainen J, Korhonen TK, Dufrêne YF. Exploring the molecular forces within and between CbsA S-layer proteins using single molecule force spectroscopy. *Ultramicroscopy*. 2007;107:1004-11.
92. Tang J, Ebner A, Ilk N, Lichtblau H, Huber C, Zhu R, Pum D, Leitner M, Pastushenko V, Gruber HJ, Sleytr UB, Hinterdorfer, P. High-affinity tags fused to S-layer proteins probed by atomic force microscopy. *Langmuir*. 2008;24:1324-29.
93. Tang J, Ebner A, Badelt-Lichtblau H, Völlenklee C, Rankl C, Kraxberger B, Leitner M, et al. Recognition imaging and highly ordered molecular templating of bacterial S-layer nanoarrays containing affinity-tags. *Nanoletters*. 2008;8:4312-9.
94. Habibi N, Pastorino L, Caneva Soumetz F, Sbrana F, Raiteri R, Ruggiero C. Nanoengineered polymeric S-layers based capsules with targeting activity. *Colloid Surface B*. 2011;88:366-72.
95. Györvary ES, Stein O, Pum D, Sleytr UB. Self-assembly and recrystallization of bacterial S-layer proteins at silicon supports imaged in real time by atomic force microscopy. *J Microsc*. 2003;212:300-6.
96. Fagan RP, Albesa-Jové D, Qazi O, Svergun DI, Brown KA, Fairweather NF. Structural insights into the molecular organization of the S-layer from *Clostridium difficile*. *Mol Microbiol*. 2009;71:1308-22.
97. Pavkov T, Egelseer EM, Tesarz M, Svergun DI, Sleytr UB, Keller W. The structure and binding behavior of the bacterial cell surface layer protein SbsC. *Structure*. 2008;16(8):1226-37.
98. Jing H, Takagi J, Liu JH, Lindgren S, Zhang RG, Joachimiak A, et al. Archaeal surface layer proteins contain beta propeller, PKD, and beta helix domains and are related to metazoan cell surface proteins. *Structure*. 2002;10:1453-64.
99. Forouhar F, Lew S, Seetharaman J, Mao L, Janjua H, Xiao R et al. Crystal structure of the surface layer protein BACUNI\_02894 from *Bacteroides uniformis*, Northeast Structural Genomics Consortium Target BtR193D, to be published.
100. Aichmayer B, Mertig M, Kirchner A, Paris O, Fratzl P. Small-angle scattering of S-layer metallization. *Adv Mater*. 2006;18:915-9.
101. Arbing MA, Chan S, Shin A, Phan T, Ahn CJ, Rohlin L, Gunsalus RP. Structure of the surface layer of the methanogenic archaean *Methanosarcina acetivorans*. *Proc Natl Acad Sci USA*. 2012;109:11812-7.

102. Arumugam K, Crouzy S. Dynamics and stability of the Metal Binding Domains of the Menkes ATPase and their interaction with the metallochaperone HAH1. *Biochem.* 2012. doi: 10.1021/bi300669e.
103. Sparta M, Shirvanyants D, Ding F, Dokholyan NV, Alexandrova AN. Hybrid dynamics simulation engine for metalloproteins. *Biophys J.* 2012;103(4):767-76.
104. Horejs C, Pum D, Sleytr UB, Tscheliessnig R. Structure prediction of an S-Layer protein by the mean force method. *J Chem Phys.* 2008;128(6):65106-11.
105. Horejs C, Mitra MK, Pum D, Sleytr UB, Muthukumar M. Monte Carlo study of the molecular mechanisms of surface-layer protein self-assembly. *J Chem Phys;* 134:125103-11.
106. Brown GE Jr, Sturchio NC. Overview of synchrotron radiation applications to low temperature geochemistry and environmental science. *Rev Mineral Geochem.* 2002;49:1-119.
107. Vyalikh DV, Kirchner A, Kade A, Danzenbächer S, Dedkov YS, Mertig M, et al. Spectroscopic studies of the electronic properties of regularly arrayed two-dimensional protein layers. *J. Phys-Condens. Mat.* 2006;18:S131-44.
108. Moll H, Stumpf Th, Merroun ML, Roßberg A, Selenska-Pobell S, Bernhard G. Time-resolved laser fluorescence spectroscopy study on the interaction of curium (III) with *Desulfovibrio äspöensis* DSM 10631T. *Environ Sci Technol.* 2004;8:1455-9.
109. Rustenholtz A, Billard I, Duplatre G, Lützenkirchen K, Sémon L. Fluorescence spectroscopy of U(VI) in the presence of perchlorate ions. *Radiochimica Acta.* 2001;89:83-9.
110. Ferner-Ortner-Bleckmann J, Huber-Gries C, Pavkov T, Keller W, Mader C, Ilk N, Sleytr UB, Egelseer EM. The high-molecular-mass amylase (HMMA) of *Geobacillus stearothermophilus* ATCC 12980 interacts with the cell wall components by virtue of three specific binding regions. *Mol Microbiol.* 2009;72:1448-61.
111. Knoll W, Naumann R, Friedrich M, Robertson JWF, Lösche M, Heinrich F et al. Solid supported lipid membranes: New concepts for the biomimetic functionalization of solid surfaces. *Biointerphases.* 2008;3:125-35.
112. Handrea M, Sahre M, Neubauer A, Sleytr UB, Kautek W. Electrochemistry of nano-scale bacterial surface protein layers on gold. *Bioelectrochemistry.* 2003;61:1-8.
113. Zafiu Ch, Trettenhahn G, Pum D, Sleytr UB, Kautek W. Electrochemical control of adsorption dynamics of surface layer proteins on gold. *Phys Chem Chem Phys.* 2011;13:3478-83.
114. Delcea, M. Bioengineering biomimetic membranes: combining S-layer technology, polyelectrolyte multilayers and lipids. Departamento de Ingeniería Química y del Medio Ambiente. Bilbao, Universidad del País Vasco. PhD; 2009.
115. Lu, JR et al. Adsorption of dodecyl sulphate surfactants with monovalent metal counterions at the air/water interface studied by neutron reflection and surface tension, *J. Colloid Interface Sci.* 1993;158:L303-16.
116. Sara M, Egelseer EM. In: Crystalline Bacterial Cell Surface Proteins. Sleytr UB, Messner P, Pum D and Sára M. editors Academic Press. 1996;103-131.
117. Messner P. Chemical Composition and Biosynthesis of S-Layers. In: Crystalline Bacterial Cell Surface Proteins. Sleytr, UB, Messner P, Pum, D. and Sára M. Academic Press. 1996;35-76.
118. Mobili P, Londero A, Roseiro T, Eusebio E, De Antoni GL, Fausto, R, Gómez-Zavaglia, A. Characterization of S-Layer Proteins of *Lactobacillus* by FTIR Spectroscopy and Differential Scanning Calorimetry. *Vibrat Spectrosc.* 2009;50:68-77.
119. Jankowski U, Merroun M, Selenska-Pobell S, Fahmy K. S-Layer protein from *Lysinibacillus sphaericus* JG-A12 as matrix for Au-III sorption and Au-nanoparticle formation. *Spectroscopy.* 2010;24:177-81.

120. Gerbino E, Mobili P, Tymczyszyn EE, Frausto-Reyes C, Araujo-Andrade C, Gómez-Zavaglia A. Use of Raman spectroscopy and chemometrics for the quantification of metal ions attached to *Lactobacillus kefir*. *Appl Microbiol*. 2012;112(2):363-71.

© 2013 Mobili et al.; This is an Open Access article distributed under the terms of the Creative Commons Attribution License (<http://creativecommons.org/licenses/by/3.0>), which permits unrestricted use, distribution, and reproduction in any medium, provided the original work is properly cited.

*Peer-review history:*

*The peer review history for this paper can be accessed here:*

<http://www.sciencedomain.org/review-history.php?iid=192&id=3&aid=960>